Energy and Buildings 85 (2014) 445–457

Contents lists available at ScienceDirect

Energy and Buildings

journal homepage: www.elsevier.com/locate/enbuild

# Effects of furniture and contents on peak cooling load

Paul Raftery [a,*], Edwin Lee [b], Tom Webster [a], Tyler Hoyt [a], Fred Bauman [a]

[a] Center for the Built Environment, University of California Berkeley, Berkeley, CA, USA
[b] National Renewable Energy Laboratory, Golden, CO, USA

ARTICLE INFO

*Article history:*
Received 23 July 2014
Received in revised form
18 September 2014
Accepted 25 September 2014
Available online 13 October 2014

*Keywords:*
Cooling load
Internal mass
Furniture
Simulation
EnergyPlus

ABSTRACT

We assess the impact that furniture and contents (i.e. internal mass) have on zone peak cooling loads using a perimeter zone model in EnergyPlus across 5400 parametric simulation runs. The zone parameters were HVAC system type (overhead, underfloor, and thermally activated building system (TABS)), orientation, window to wall ratio, and building envelope mass. The internal mass parameters were the amount, area, and the material type used. We also evaluated a new internal mass modeling method, which models direct solar radiation on the internal mass surface, an effect that is missing in current methods. We show how each of these parameters affect peak cooling load, highlighting previously unpublished effects. Overall, adding internal mass changed peak cooling load by a median value of −2.28% (−5.45% and −0.67% lower and upper quartiles respectively) across the studied parameter space. Though the median is quite low, this study highlights the *range* of effects that internal mass can have on peak cooling loads depending on the parameters used, and the discussion highlights the lack of guidance on selecting reasonable values for internal mass parameters. Based on this we recommend conducting an experimental study to answer outstanding questions regarding improved specification of internal mass parameters.



## 1. Introduction

Whole-building energy simulation is a widely used method to design and evaluate the energy performance of a building. The peak cooling load in each thermal zone in the model is often a key aspect of design, as it determines the size of the HVAC equipment needed to cool the zone sufficiently, which has affects energy performance throughout the year. It also influences the peak demand of the building.

A wide range of factors affect the peak cooling load in a thermal zone, such as:

- Solar radiation through fenestration;
- Transient conduction through zone surfaces;
- Internal gains (convective and radiant) from occupants, lights and equipment;
- Infiltration;
- The capacitive effects of the zone air volume;
- The HVAC system used to reject heat from the zone;
- The thermal inertia of the furniture and contents (internal mass).

This paper focuses on the effect that internal mass has on cooling loads, and how current simulation tools model these effects. There is considerable debate whether current practices yield sufficiently accurate instantaneous peak cooling load estimates. This also applies to heating loads, but is less critical because heating energy costs are not as time and peak sensitive as cooling energy costs.

Currently, the most detailed method to estimate these loads is to use a whole building energy simulation tool that assesses all aspects of heat exchange within a building simultaneously, and which captures temporal effects related to thermal inertia of the building elements. As with any simulation-based approach, simplifications and assumptions are necessary to reduce the complexity of the model. This ensures that the detail of the input parameters and the run-time of the simulation remain feasible for the particular application. This paper assesses how peak cooling loads are affected by internal mass and also discusses the effect of simplifications regarding current modeling methods in whole building energy simulation tools, and in particular, EnergyPlus.

### 1.1. Review of the surface heat balance

Modern whole-building energy simulation programs typically perform a detailed heat balance calculation at each surface in the model. The various heat transfer components within a thermal zone

* Corresponding author at: Center for the Built Environment, University of California, 390 Wurster Hall, Berkeley, CA 94720-1839, USA. Tel.: +1 510 643 6915.
*E-mail addresses:* p.raftery@berkeley.edu, research@paulraftery.com (P. Raftery).

http://dx.doi.org/10.1016/j.enbuild.2014.09.081
0378-7788/

are comprehensively described in [1] and briefly reviewed here. The major components of heat transfer at each surface are:

- *Conduction*: Transient conductive heat transfer through a surface (either to the exterior environment or to other zones in the model) is often modeled using a transfer function or response factor approach [2], although some simulation programs, including EnergyPlus [3] also include a finite difference model as well. Any heat sources or sinks at depth within the surface (such as hot or cold water in hydronic tubing such as in a thermally active building system) also affect conductive heat transfer through the surface.
- *Short-wave radiation*: This is primarily due to solar radiation entering the zone through fenestration and typically has two components: direct and diffuse radiation. Whole-building energy simulation tools sometimes model direct solar radiation illuminating many zone surfaces, but often only the floor as a simplification. These methods avoid a detailed solar distribution calculation for each surface in the zone. Typically, the tools uniformly apply diffuse radiation (that either has entered through fenestration or has been scattered from direct solar radiation on zone surfaces) to surfaces using a surface area weighted average. The short-wave radiant component of lighting loads is typically added to the diffuse radiation.
- *Long-wave radiation*: Long-wave radiant exchange between surfaces in the zone is modeled using the temperatures of those surfaces, their emissivity, and calculated surface view factors. Long-wave radiative components of internals loads such as lighting, occupants, and equipment are typically applied uniformly across all surfaces using a surface area weighting.
- *Convection*: Convection from a surface is determined based on orientation, surface roughness, surface temperature and air temperature.

### *1.2. Review of the zone air heat balance*

The combined result of the heat balance calculation at each surface lead to a heat balance for the zone air. Starting with the assumption that zone air is fully mixed, and adequately represented by a single temperature node, the rate of change of the zone air temperature is determined based on the following:

- The sum of the convective heat gains (or losses) from the surfaces in the zone;
- The convective components of the internal loads;
- The capacitance of the zone air and the amount of infiltration;
- The amount of heat removed (or added) by the air HVAC system.

The instantaneous cooling load of a zone is defined as the total cooling power required to maintain the zone air at the cooling setpoint temperature. For a all-air HVAC system, when the zone air is at the cooling set point, the cooling load the heat gained between the supply air and the return air. Two components comprise the cooling load for a thermally active building system (TABS) – the heat absorbed by the TABS element (e.g. the heat gained between the supply and return water in a hydronic slab system) and the heat gained between the supply air and the return air (the secondary ventilation air system).

### *1.3. Current methods for modeling internal mass*

It is important to clarify a key point about internal mass modeling before continuing this discussion. In older simulation tools, or in studies that use simplified resistance-capacitance network modeling approaches, internal mass objects often represent structural building elements (such as floor slabs and other structural elements) as well as furniture and contents. This was necessary due to the broader assumptions and simplifications used in these tools regarding heat transfer, namely that they did not separately account for the thermal inertia of these structural elements. However, internal mass only represents furniture and contents in more modern tools (e.g. EnergyPlus and ESP-r) as these tools do capture the thermal inertia of structural elements. In this paper we assume internal mass refers to only the furniture and contents in the building, and that major elements of the building – the floors, walls and ceilings that separate discrete thermal zones – are explicitly modeled independently of the internal mass object.

Traditionally, internal mass within zone heat balance calculations has been implemented using a simplified approach where the internal mass occupies the zone without regard to the shape or location of the furniture (i.e. the geometry). Following on from mathematical studies focused on this topic [4], numerous experimental [5] and simulation based studies [6–11] have been performed on how thermal mass can be designed to minimize energy use in a building. Internal mass within zones has been modeled using a lumped thermal network approach used as part of an inverse modeling process that uses a parameter estimation technique to determine internal mass thermal properties from experimental data [12]. Some studies use an inverse approach in which ideal thermal properties of building materials are evaluated in order to minimize the energy usage of a building [13], which is in contrast to a typical building simulation process that involves specifying building and mass material properties. Although there are a range of modeling approaches used in the simulation studies, one common factor is that all of them use a simplified internal mass model that does not account for geometry. These studies also use a single node (or at most two nodes) to represent all the thermal mass within a zone (or often even the whole building), including the furniture (where this is explicitly mentioned in the study), internal walls, floors, and ceilings.

Within EnergyPlus [14], an internal mass object consists of a defined construction (a one-dimensional set of discrete layers, each with separate thermal properties) and an exposed surface area that interacts with the zone heat balance on one side of the surface and has an adiabatic boundary condition on the other side. Because this is not a geometric description, direct solar radiation illuminates the zone surfaces in the model but not the thermal mass surface. Aside from this difference, EnergyPlus accounts for all elements of the surface heat balance method described in Section 1.1 for each internal mass surface exactly as it would for any other surface in the model.

### *1.4. Problem statement*

We start from the assumption that the model in question explicitly represents each of the surfaces enclosing a thermal zone independently. Internal mass then solely refers to the furniture and contents in a zone. As described in Section 1.3, all of the approaches to date use a geometrically simplified internal mass, even when described independently from other surfaces within the zone. This is because it is generally intractable to consider furniture in a detailed fashion in a whole-building energy simulation environment. Under the current assumptions of the most detailed modeling engines, internal mass interacts with: (a) the zone air through convection, (b) diffuse radiation in the zone assuming a uniform surface area weighted exchange, (c) long-wave radiation exchange assuming a uniform surface area weighted exchange. We assume that each of these approaches is valid, appropriately detailed representations of the underlying processes given current limits to computing capabilities. The missing piece in this representation is an approach that couples the internal mass to direct solar radiation, and considers the partial shading of the floor underneath.

The authors believe that a modeling approach that considers these effects more accurately represents heat transfer within the zone.

We propose a new method to model this effect (referred to as the "Geometric" mass case) and present the results of testing it under a range of different conditions in this paper. We chose EnergyPlus as the simulation tool for this research as it is one of the most capable energy simulation tools available today [15], has been extensively validated [16], and models all aspects of the zone and surface heat balance calculations described in Sections 1.1 and 1.2.

## 2. Description of the proposed geometric mass modeling method

The two main aims of this new method are: (a) to account for the effect of direct solar radiation on internal mass, and (b) to shade other surfaces in the zone accordingly. We expected this modeling method to show a larger effect for HVAC systems that have a large temperature asymmetry within the zone, particularly those with inherently lower surface temperatures. For example, consider an Under Floor Air Distribution (UFAD) system. Solar radiation on the raised floor affects the temperature of air supplied through the supply air plenum [17]. Thus, it is essential to model the solar radiation component realistically. As it currently stands with the existing method, solar gain illuminates the entire floor surface. Furniture has no shading effect (as it does in a real building) and this overestimates the heat flow into the supply air through the raised floor. Likewise, for a TABS case, such as a slab that is cooled using hydronic tubing, direct solar radiation on the floor affects the cooling capacity of the slab.

### 2.1. Direct solar radiation

When direct solar radiation enters a zone, the portion of floor area illuminated by that radiation is a function of the placement and shape of objects in the zone. It is generally intractable to consider these in a detailed fashion in a building energy simulation environment, but a simplified geometry can be used to represent the furniture and more accurately consider the internal mass in the zone. In the new method, a single horizontal surface in a zone represents the furniture. This ensures that direct solar radiation interacts with the internal mass object, as it does with furniture in a real building. This is a simplification but it serves as a useful first approximation to evaluate whether or not the exposure of internal mass to direct solar will have an effect. We varied the amount of internal mass and the exposed surface area in this study as described later in Section 3.5.2. To reduce the number of simulation runs, we fixed the height of the surface at 0.5 m. We also fixed the location of the geometric mass in the center of each zone. Placement in this orientation allows exposure of a proportionally similar amount of the mass throughout the diurnal cycle in the east and west facing zones, reducing any bias introduced with this implementation.

As well as adding an additional surface to the model, we also split the floor surface into three surfaces. This multiple floor surface approach allows a portion of the solar radiation to be directly incident on two floor surfaces, while shading the other subsurface. The centermost surface is directly below the geometric mass surface, where it is fully shaded from direct solar radiation. This simplification approximates the shading effect of furniture as it occurs in a real building. The effect of direct solar on floor surfaces on cooling load has been discussed in recent research [18,19], as has the floor shading effect caused by furniture [20].

The EnergyPlus model used in this research (described in Section 3) uses the Full Interior And Exterior modeling approach. As stated in the EnergyPlus documentation, this approach "...calculates the amount of beam radiation falling on each surface in the zone, including floor, walls and windows, by projecting the sun's rays through the exterior windows..." Implementing the geometric modeling method required minor modifications to the EnergyPlus source code to ensure that (a) the mass surface is exposed to direct solar radiation and (b) that the floor surface directly underneath the mass surface is shaded from direct solar radiation.

### 2.2. Long wave radiation exchange

The geometric mass surface also exchanges long wave radiation based on the view factor to other surfaces within the zone. This is different from the existing method that assumes uniformly distributed long wave radiative heat transfer weighted by surface area within the zone. Thus, it is necessary to split the geometric mass surface into two, with one facing upwards and the other facing downwards, in order to capture a more reasonable 'average' view factor which is similar to that used for the existing internal mass object, and more representative of furniture in a real building. Each of the two mass surfaces in the geometric mass method interact with the zone on one side only (the other side is adiabatic as is the case for the existing method) and we assume that there is no direct solar radiation on the lower surface. The total area of the two geometric mass surfaces matches the area of the mass surface using the existing method, as does the thickness of the each mass surface.

## 3. Method

We used a full factorial parametric study to examine how peak loads vary across a broad set of scenarios typically found in buildings. We also investigated the effects of using the new method (described in Section 2) for modeling internal mass instead of the existing method. To do this, we simulated a zone using a wide range of parameters, and assessed this for the following three different HVAC systems:

1. a traditional Variable Air Volume (VAV) overhead system representing a fully mixed zone;
2. an Under Floor Air Distribution (UFAD) system representing a thermally stratified zone, and
3. a radiant hydronic slab system representing a system in which the building's structural mass directly interacts with the HVAC system (e.g. a thermally active building system – TABS).

### 3.1. Geometry

The model represents a perimeter zone in a large multi-story office building. We assumed one exterior facade (with a window) exposed to exterior conditions. The other walls in the model represent interior walls between other zones in the building that we assumed to be at the same temperature and thus we used an adiabatic boundary condition for these walls. To represent intra-floor heat transfer the floor and ceiling are thermally connected.

The occupied space has an identical volume in both the UFAD and OH models: 25 m long by 5 m wide, with a floor-to-ceiling height of 2.7 m. The OH model represents this space using a single well-mixed zone, whereas the UFAD model represents this space using a two-zone model, which captures the effects of stratification that occurs in these systems [21]. The total plenum volume is identical in both the UFAD case (where the supply and return plenums are both 0.3 m high) and the OH case (where the return plenum is 0.6 m high). We maintained a fixed floor-to-floor height when modeling the radiant hydronic slab case, which does not have a plenum.

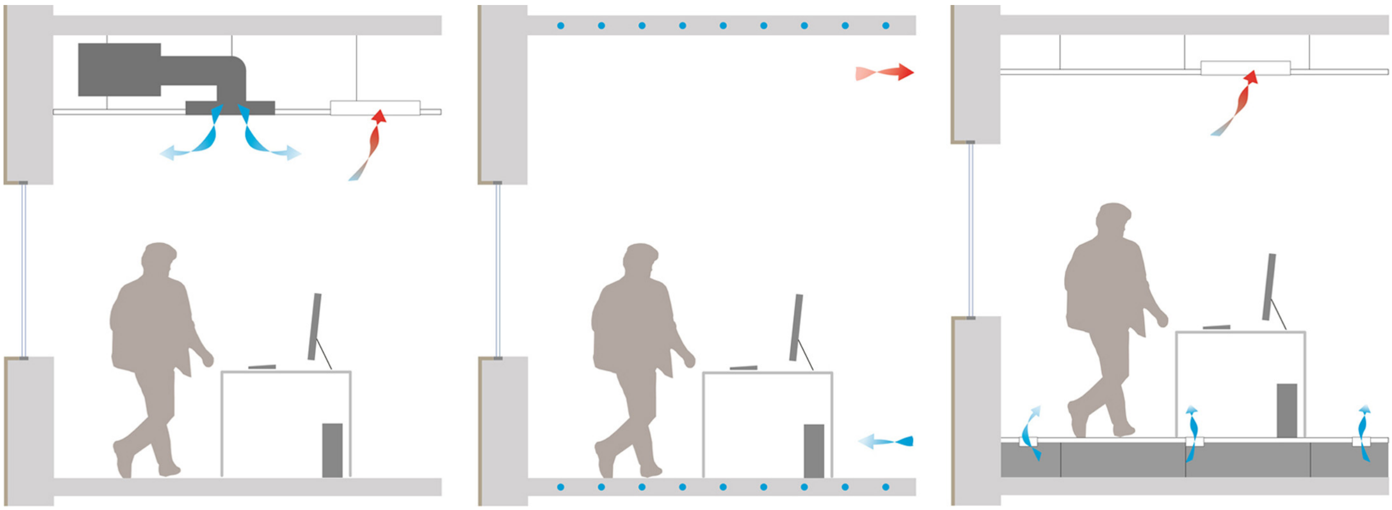

**Fig. 1.** Schematic diagram of the three HVAC systems simulated in this study. Left: Overhead (OH), Middle: Thermally Activated Building System (TABS), & Right: Underfloor Air Distribution (UFAD). Images courtesy of Caroline Karmann at the Center for the Built Environment, University of California Berkeley.

Thus, the total conditioned volume is 25 m × 5 m × 3.3 m regardless of the modeled HVAC system. Fig. 1 illustrates these three systems.

There is also one window in the zone. It spans the full length of the zone (25 m) with the bottom placed at a typical sill height of 0.91 m (36 in. in the US) from the floor of the occupied zone, except in high window-to-wall ratio (WWR) cases where the larger window would extend above the top of the occupied zone. In these cases, the bottom edge of the window is at floor level.

The materials and constructions used in the model are similar to those used in the PNNL Commercial Prototype Building models for large offices based on the ASHRAE 90.1-2010 standard. We note the thermal properties of materials that are specific to this model, such as the properties of the window and the raised floor panels. Table 1 summarizes the constructions used in the model. The whole window construction has a *U*-value of 2.85 W/m$^2$ K and a solar heat gain coefficient of 0.287, which is common across all models. There is no drop ceiling construction in the TABS case and there is no carpet in the floor slab construction for the UFAD case. Lastly, the raised floor construction is only used in the UFAD case and the concrete floor panel has the following thermal properties: 40 mm thick, 0.2359 W/m K, 1185 kg/m$^3$ with a specific heat capacity of 669 J/kg K.

### *3.2. Internal loads and infiltration*

Table 2 summarizes the internal loads used in the model which are based on ASHRAE Standard 90.1 [22]. The lights are assumed to be surface mounted and the values for the radiant and visible fractions were based on IESNA values [23]. We used a value for infiltration of 0.57 mm/s (infiltration represented as volumetric flow rate per exterior surface area) with a linear wind velocity coefficient of 0.224. These values were taken from the DOE benchmark building models, which have been recently updated by researchers at the Pacific Northwest National Laboratory [24].

**Table 2**
Description of the internal loads used in the model.

| Load type | Load level | Radiant fraction | Visible fraction |
|---|---|---|---|
| Occupants | 18.6 m$^2$/person | 0.4 | – |
| Equipment | 10.8 W/m$^2$ | 0.5 | – |
| Lighting | 9 W/m$^2$ | 0.72 | 0.18 |

### *3.3. Weather data*

For this study, we used TMY3 data for the San Francisco International Airport using 99% heating and 1% cooling design days. We chose this location as it was based in California (a restriction related to the project funding) and because the outdoor temperature on the cooling design day varies above and below the cooling set-point. This means that the exterior environment cools the building during the night and heats it during the day, and thus the transient effects related to thermal inertia will be apparent. Performing this analysis in a much warmer climate with cooling design day temperatures that are always above the cooling set-point, such as Sacramento, would mean that the building would always operate at the cooling set-point and that the thermal mass would not significantly change temperature throughout the design day. We obtained the design day weather conditions from the EnergyPlus Weather Data website [25]. To summarize, on the cooling design day the outside air dry-bulb temperature varies over a range of 8.5 °C and reaches a maximum temperature of 25.7 °C, and the direct solar radiation reaches a peak value of 890 W/m$^2$. We used the same design day for every simulation run.

**Table 1**
Description of the materials and constructions used in the model.

| Construction | Outer material layer | Center material layer | Inner material layer |
|---|---|---|---|
| Interior wall | 12.7 mm (½ in.) gypsum wall board | Air gap | 12.7 mm (½ in.) gypsum wall board |
| Heavy-weight exterior wall | 200 mm (8 in.) concrete | 40 mm (1½ in.) expanded polystyrene insulation | 12.7 mm (½ in.) gypsum wall board |
| Light-weight exterior wall | Aluminum/Steel siding (0.11 m$^2$K/W) | 40 mm (1½ in.) expanded polystyrene insulation | 12.7 mm (½ in.) gypsum wall board |
| Drop ceiling | 12.7 mm (½) ceiling tile | – | – |
| Floor slab | 150 mm (6 in.) concrete | – | Carpet (0.217 m$^2$K/W) |
| Raised floor | Concrete raised floor panel | – | Carpet (0.217 m$^2$K/W) |
| Window | 6 mm (¼ in.) clear glass | 6 mm (¼ in.) air gap | 6 mm (¼ in.) clear glass |

### 3.4. Set-points and miscellaneous other inputs

The zone heating and cooling set-points are 21 °C and 24 °C respectively, with a 2 °C setback from 6 pm to 7 am. The model uses a constant supply air temperature set-point of 17 °C for the UFAD & TABS cases, and 14 °C for the OH case. The chilled water temperature used to cool the slab in the TABS case is 15 °C. The control point for each system is the same as is typically used in practice: the overhead system controls the mean air temperature in the zone, the UFAD system controls the air temperature at the thermostat height in the occupied sub-zone, and the TABS system controls to the mean operative temperature in the zone. The model uses a 5-min zone time-step.

### 3.5. Parameters varied in the simulations

#### 3.5.1. Zone level

We evaluated the impact of internal mass and the internal mass modeling method over a wide range of load conditions typically found in office buildings. We used the following parameters:

- HVAC system: UFAD, overhead (OH), TABS.
- Zone orientation: North (N), South (S), East (E), and West (W).
- Window to wall ratio: 0.2, 0.4 and 0.6.
- Building envelope thermal mass: light and heavy.

#### 3.5.2. Internal mass

We then added parameters related to internal mass itself, as there is very little guidance regarding this in existing literature (as discussed later in Section 5.1):

- *Type of internal mass*: No internal mass (“None” – for context), internal mass modeled using the existing object within EnergyPlus (“Existing”), and internal mass modeled as described above (“Geometric”).
- *Mass material*: wood or concrete.
- *Amount of mass per total zone floor area*: 25 kg/m$^2$, 50 kg/m$^2$, 100 kg/m$^2$, 200 kg/m$^2$, 250 kg/m$^2$ or 300 kg/m$^2$.
- Floor Area Coverage (FAC), or the percentage of total zone floor area covered by the mass surface: 0.3, 0.6, 0.9.[1,2]

Clearly many more parameters could affect the impact that both the amount of internal mass and the modeling method have on peak cooling loads. To give a non-exhaustive set of examples:

- *Climate related* – the range of diurnal temperature variation, and the size of the difference between the lowest outdoor air temperature and the cooling set-point on the design day.
- *Building related* – zone aspect ratio, shape & size.
- *Envelope related* – the insulation properties of the exterior wall, and the infiltration rate.
- *Internal load related* – the level and schedules for occupants, lighting, and equipment.
- *Constructions* – other interior and exterior wall constructions, other types of windows.

[1] Several of the parameters regarding the internal mass could be described differently. For example, the study could vary the thickness and the amount of mass per area, instead of the amount of mass and the floor area coverage percentage. Both would give a wide range of internal mass in the models. We decided to use the mass per floor area and FAC representation because it has been described that way in existing literature [26].

[2] We split the floor surface into three parts (according to floor area coverage percentage) in the no mass cases too. This was to ensure that the only difference between a no internal (“None”) mass case and an otherwise identical case with internal mass, were the parameters solely related to the internal mass.

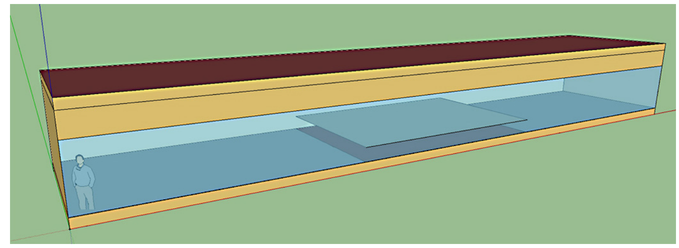

**Fig. 2.** Screenshot from OpenStudio's SketchUp plugin showing one of the models with a UFAD HVAC system, 60% window to wall ratio, and geometric mass (30% FAC). Interior surfaces exposed to direct solar radiation are highlighted in light blue.

- *Material properties* – surface emissivity and reflectivity.
- *Control related* – the cooling set-point schedule (if not held constant).
- *Simulation assumptions* – radiant fraction of internal loads.

We chose to vary parameters that would affect the cooling load over the wide range of load and mass conditions typically found in buildings, while still yielding a feasible number of total simulations. The combined set of parameter values yields 5400 individual simulation runs.

Lastly, to help visualize what we simulate in this paper, Fig. 2 shows an example of one of the models with a UFAD HVAC system, 60% window to wall ratio, and the “Geometric” mass case (30% FAC). The supply and return plenums are visible, along with the geometric mass and the shaded floor surface (directly underneath the mass surface).

## 4. Results

The title of each of the following figures describes the subset of the parameter space presented in that figure. The first line describes the restrictions placed on the zone level parameters. e.g. “UFAD, S, 0.4 WWR”, means that the figure represents data from a subset of simulations which use a UFAD HVAC system, where the zone is South facing and the window-to-wall ratio is 40%. The second line describes the restrictions placed on the parameters solely related to the internal mass. For example, “100 kg/m$^2$, 60% FAC, Wood” means that the figure represents data from a subset of simulations where the internal mass is 100 kg/m$^2$, covering 60% of the total floor area, and has the material properties of wood. The third line shows ‘*n*’, the number of runs in that particular subset, and a description of the what data the figure presents. For example, “*n*: 2, Radiation incident on the mass surface”.

It is not feasible to represent the results from each run in detail visually using time-series data due to the sheer quantity of data. However, for illustration purposes we first present time-series results for small subsets of runs in Sections 4.1 and 4.2. We then use aggregate visualization methods (boxplots) to present the results over the entire parameter space in Section 4.3.

### 4.1. Validating the source code changes for the geometric mass model

First, we verified that the distribution of direct solar radiation is correct within the zone when using the new geometric method for modeling internal mass. We checked that direct solar radiation illuminates the mass surface using the geometric method, and does not using the existing method. We also verified that the centermost floor surface (directly underneath the internal mass surface) is shaded in the “Geometric” case and is not shaded in the “Existing” case. Lastly, we also summed the solar radiation heat gain (both direct and diffuse) over all zone surfaces in both models to verify that they are the same for both the geometric, existing, and no internal mass cases. This showed that the modified EnergyPlus source code functioned correctly and it is not double accounting for solar load in the model. We performed these comparisons automatically (using an R script) to ensure that the same applies across all of the simulation runs. In addition to these tests, we also assessed numerous other variables (such as the distribution of diffuse radiation within the zone, total surface convection, heat storage rates within the surfaces, etc.) for each of the models, however, these are not discussed here for the sake of brevity.

### *4.2. Demonstrating the influence of the model parameters*

Next, we present the difference between the results of the two approaches for modeling internal mass (with a no mass case for additional context) over a subset of the runs to demonstrate the influence that the studied parameters have on the results. We do this because many of these observations have not been studied to date. For illustration purposes, we present the results for a relatively extreme case (high mass, high area, etc.) and present quantitative results over the entire parameter space later in the paper, in Section 4.3.

#### *4.2.1. The effect of window to wall ratio and orientation*

Fig. 3 highlights that orientation plays a major role in both the magnitude of the cooling load and the time at which it occurs. It also shows that adding internal mass delays the occurrence and magnitude of peak cooling load. The figure shows that the geometric modeling method tends to decrease peak cooling loads further

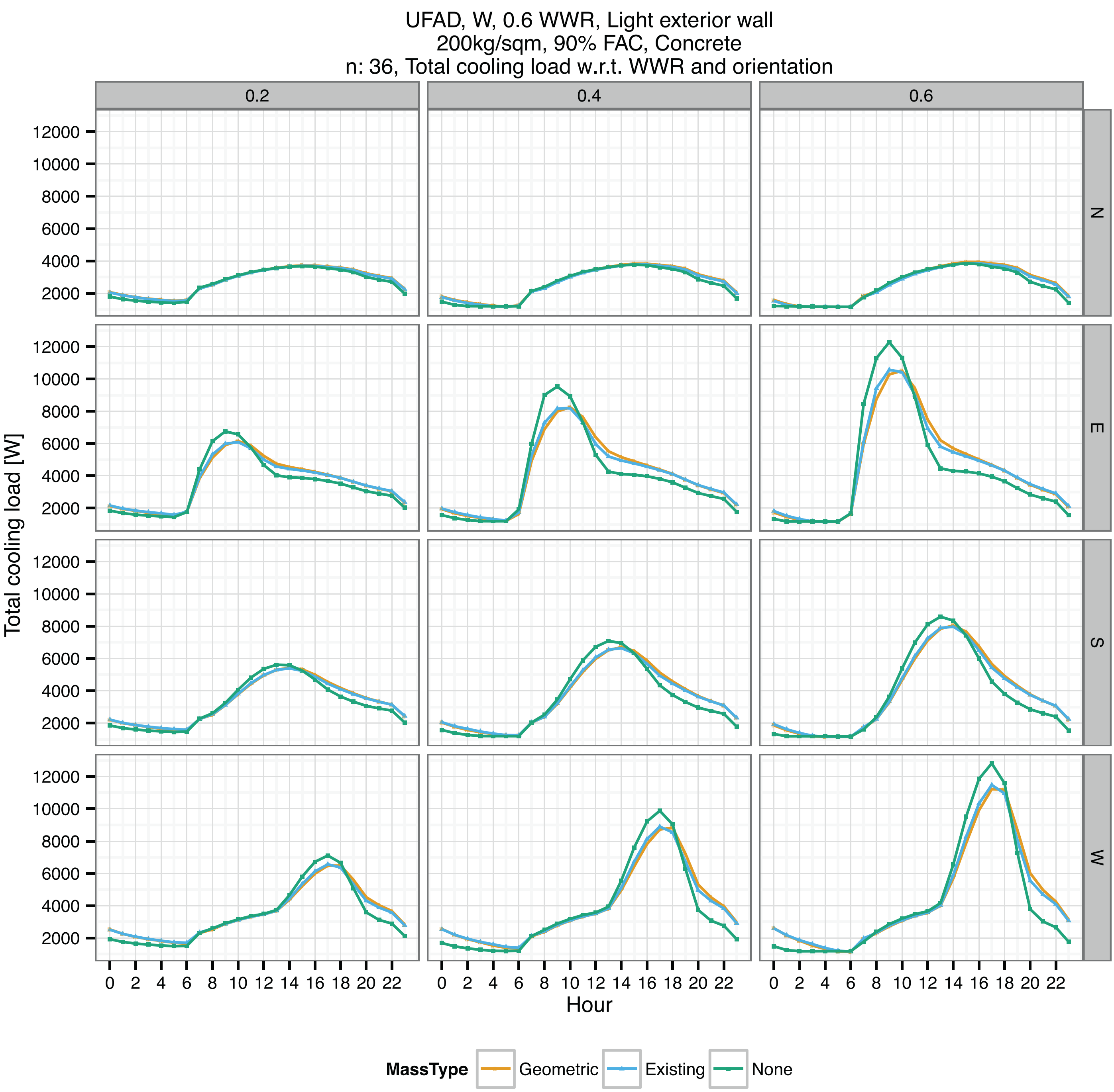


**Fig. 3.** Time-series data showing the instantaneous cooling load on the cooling design day with respect to window to wall ratio and orientation.

when compared to the existing method. This is because of the exposure of the internal mass to direct solar radiation in the "Geometric" case, and not in the "Existing" case. For an identical amount (and area) of internal mass this difference increases how much the mass interacts with loads in the zone. Internal mass generally reduces peak cooling loads when compared to a no mass case, so when the internal mass interacts more with the loads in the space, further reduction of the loads occurs. The figure also shows that the magnitude of this effect increases in zones with high solar gain (e.g. east and west zones, and zones with larger window to wall ratios).

### 4.2.2. Effect of exterior wall type

Even when the insulation layer of the exterior wall is the same, the material properties of other layers in the exterior wall also affect peak cooling loads. Zones with heavy-weight exterior walls have lower peak cooling loads than an identical zone with a light-weight exterior wall. However, the effect of internal mass on cooling loads is largely independent of whether or not the exterior wall is light- or heavy-weight.

### 4.2.3. Effect of internal mass material type

Fig. 4 shows the impact of the material chosen for the internal mass. Materials with higher thermal conductivities and specific heat capacities have a larger impact on the results. The property of thermal diffusivity captures this effect comprehensively. It measures the ability of a material to conduct thermal energy relative to its ability to store thermal energy. Defined as the ratio of thermal conductivity to volumetric heat capacity, diffusivity has units of meters squared per second. Values for a wide range of materials and their application in low energy buildings is described in existing publications [10]. Comparing the thermal diffusivity of concrete (0.892 $mm^2/s$) and wood (0.183 $mm^2/s$) indicates why concrete has a larger impact for the same mass despite its lower specific heat capacity. For the materials that furniture and contents typically consist of (mostly wood, paper, plastic), the current practice of assuming wood as the internal mass material type appears to be a reasonable assumption. However, some modelers include intrazone surfaces between zones with similar temperatures in their estimates for internal mass and in some cases, these surfaces are made of concrete. For example, the structural walls around the services zone in the core of a building, or concrete walls in legal offices. For these cases, the best representation for the internal mass material is likely to lie in between the properties of wood and concrete.

### 4.2.4. Effect of Floor Area Coverage and amount of mass

Fig. 5 shows that increasing amounts of internal mass have a larger effect on peak cooling loads, as one would expect. The effect of varying Floor Area Coverage (FAC), that is, the spread of the internal mass over the interior space, is more complicated than the other parameters. This is because the thickness of the internal mass surface plays a role on cooling loads, and this varies with FAC for a fixed amount of mass per area. Fig. 5 shows that peak cooling load decreases with increasing FAC for large amounts of mass, and increases with increasing FAC for a small amount of mass.

The fact that internal mass can actually increase peak cooling loads is a counterintuitive finding not reported before, to the author's knowledge. When an internal mass surface is very thin, incident radiation causes the surface temperature to rise quickly, and thus the surface rapidly converts the radiation to a convective load. The convective loads from the other surfaces in the model remain the same (or similar) so the peak cooling load increases when compared to the no mass case. The mass in the "Geometric" case is exposed to more solar gain (i.e. direct and diffuse) than in the "Existing" case (i.e. only diffuse), and thus this effect is amplified for the geometric mass at low thicknesses. As the internal mass surface gets thicker, it can absorb more heat with less surface temperature rise, and the additional exposure to solar radiation becomes an advantage for the "Geometric" case with regard to reducing peak

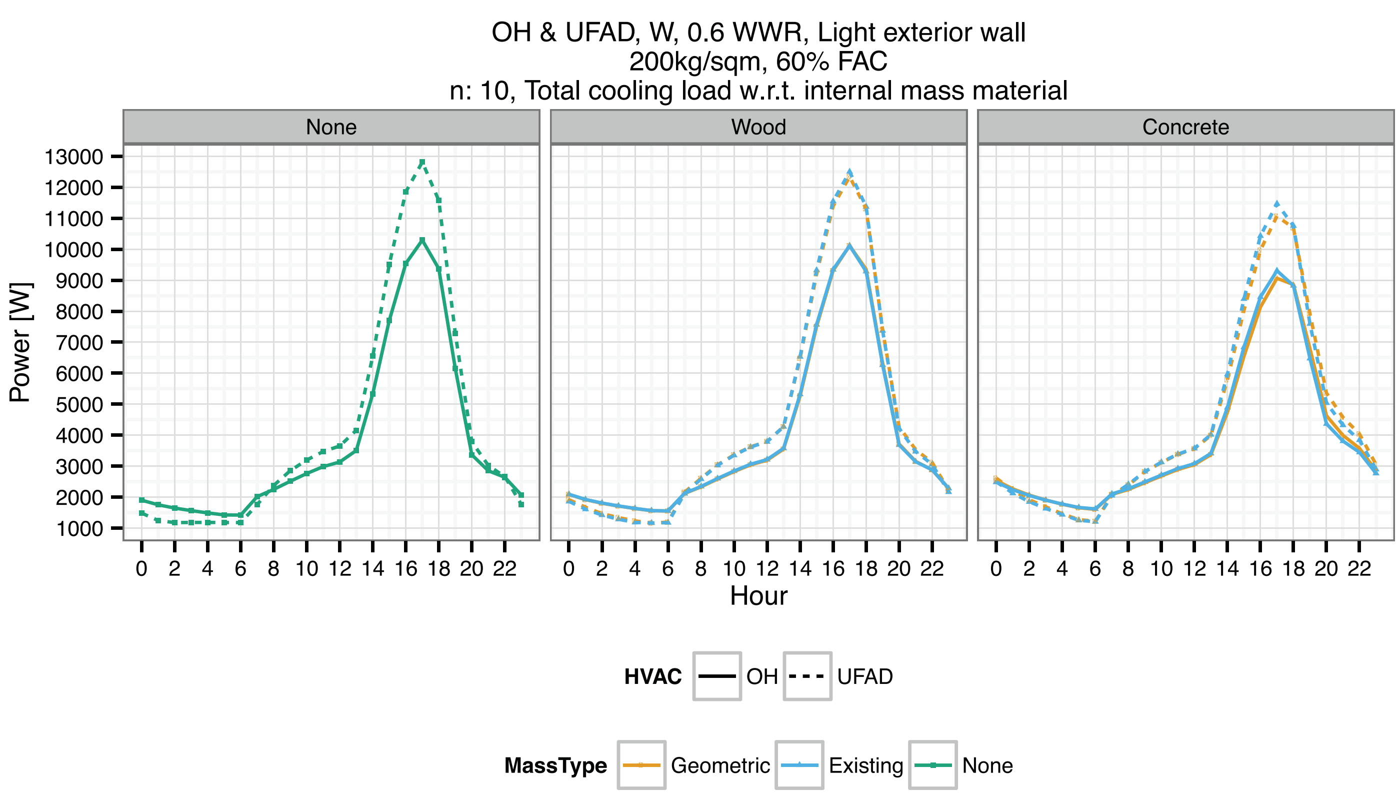


**Fig. 4.** Time-series data showing the instantaneous cooling load on the cooling design day with respect to internal mass material.

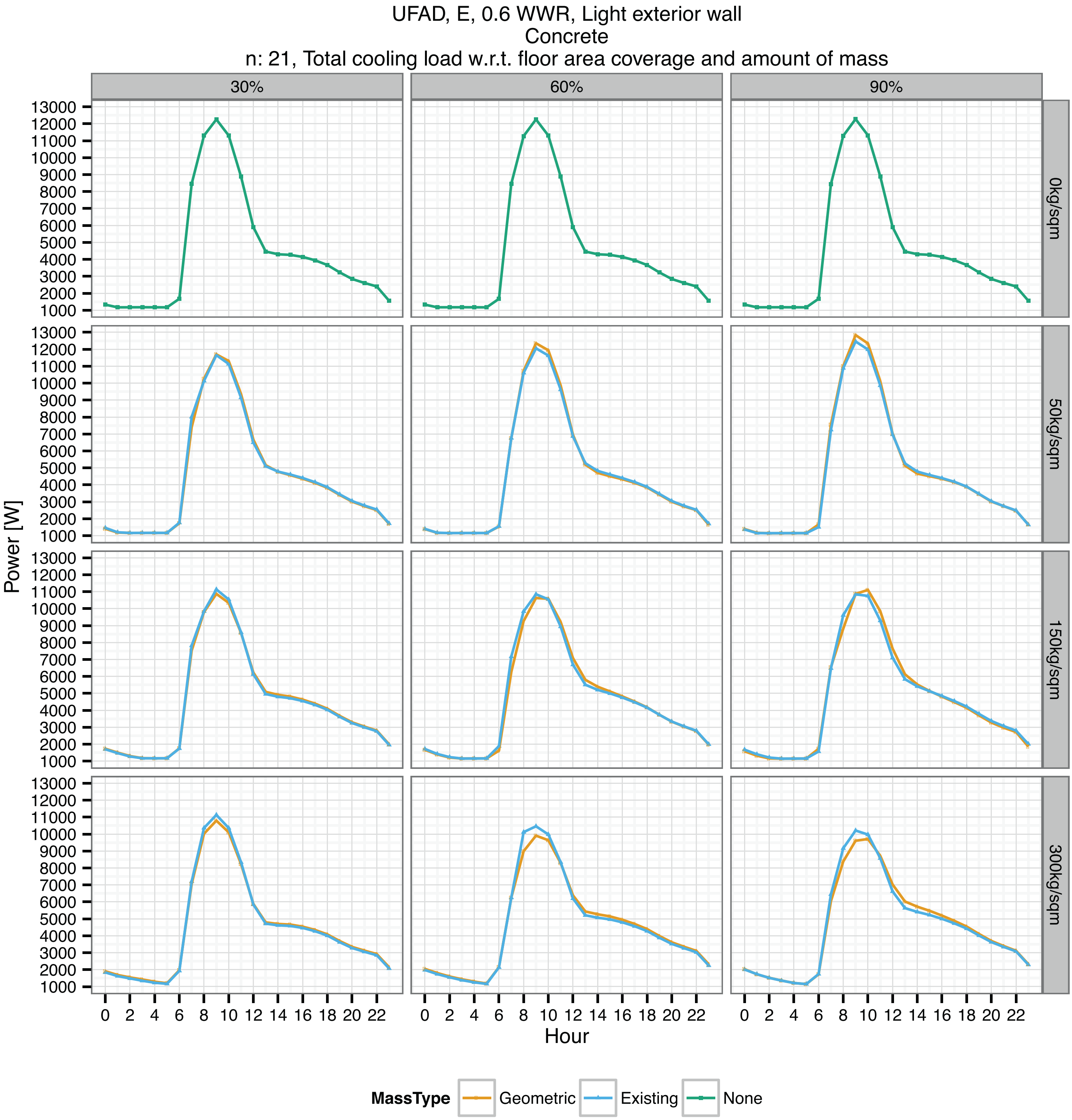


**Fig. 5.** Time-series data showing the instantaneous cooling load on the cooling design day with respect to the amount of internal mass and the fraction of floor area coverage (FAC).

cooling loads. Fig. 6 illustrates this last point clearly by holding FAC at a constant value and varying the amount of internal mass.

### 4.3. Results over the complete parameter space

The results presented in Section 4.2 represent a relatively small number of runs, which is useful for illustration purposes. It provides an understanding of the effect of various model parameters on heat transfer. However, broad-ranging conclusions drawn on a limited subset are not valid. In this section, we quantitatively present results over the whole dataset. This gives a reasonable estimate of the effect that internal mass, and the choice of modeling method has under the circumstances typically found in buildings. However, the entire parameter space includes many cases where there is little or no direct solar (e.g. a north facing zone, or a south facing zone with a low window to wall ratio). In these cases, the modeling method should have little or no impact on the results as the major difference is how the two models handle direct solar radiation. Thus, we also present the results for a large subset of the data where exposures to high levels of direct solar in the

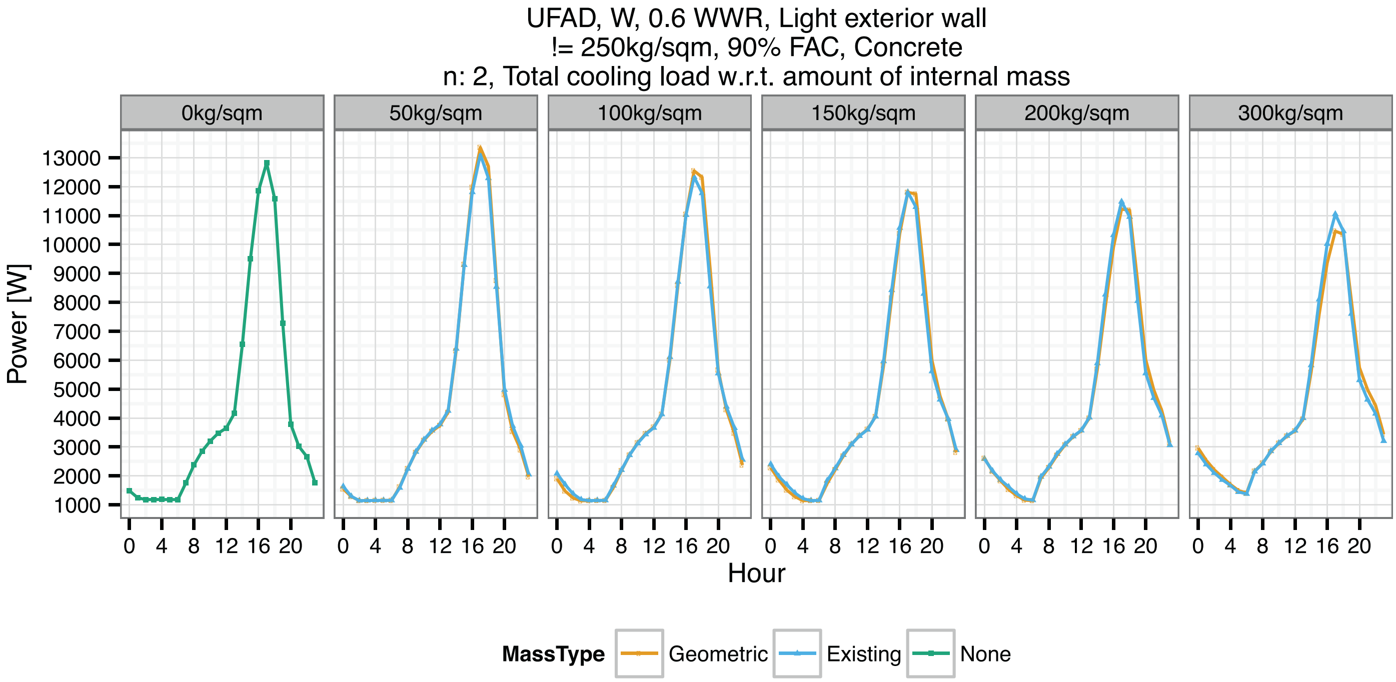


**Fig. 6.** Time-series data showing the instantaneous cooling load on the cooling design day with respect to the amount of internal mass at a constant fraction of floor area coverage (FAC).

zone (e.g. east and west facing zones with a high window to wall ratio).

#### 4.3.1. Surface temperatures

First, we look at the maximum (or peak) surface temperature reached on the cooling design day. Fig. 7 shows that modeling furniture as a geometric surface increases the peak surface temperature of the mass surface. In these cases, the mass receives direct solar radiation in the "Geometric" case, and not in the "Existing" case. Fig. 8 shows that the effect is larger for zones with higher levels of direct solar radiation (east and west facing with high window to wall ratios). However, the overall effect on *zone mean radiant temperature* is very small. The peak mean radiant temperature increased by a median value of 0.1 °C when comparing the geometric modeling method to the existing method across the entire parameter space. This is because the warmer surface temperature of the internal mass partially offsets the effect of the shaded floor, which is cooler than in the "Existing" case where the floor is not shaded.

#### 4.3.2. Cooling load

The peak cooling load found for each of the 5400 simulation runs in this study have minimum, lower quartile, median, upper quartile, and maximum values of 2.94 kW, 4.11 kW, 6.46 kW, 8.03 kW, 13.4 kW respectively. In this section, we present the results using the median value followed by the lower and upper quartiles in parentheses. Overall, we found that adding internal mass changed peak cooling load by −2.28% (−5.45%, −0.67%) across the studied parameter space. This range of values gives context to the values that follow for assessing the effect of the internal mass modeling method. We determined that applying the new "Geometric" method changed peak cooling load by −0.25% (−1.02%, +0.23%) when compared to the "Existing" method across all of the cases with mass in the studied parameter space. Fig. 9 presents this information visually using a boxplot broken out for each type of HVAC system. As clearly shown, there is little difference between the "Geometric" and "Existing" cases when evaluated across the entire

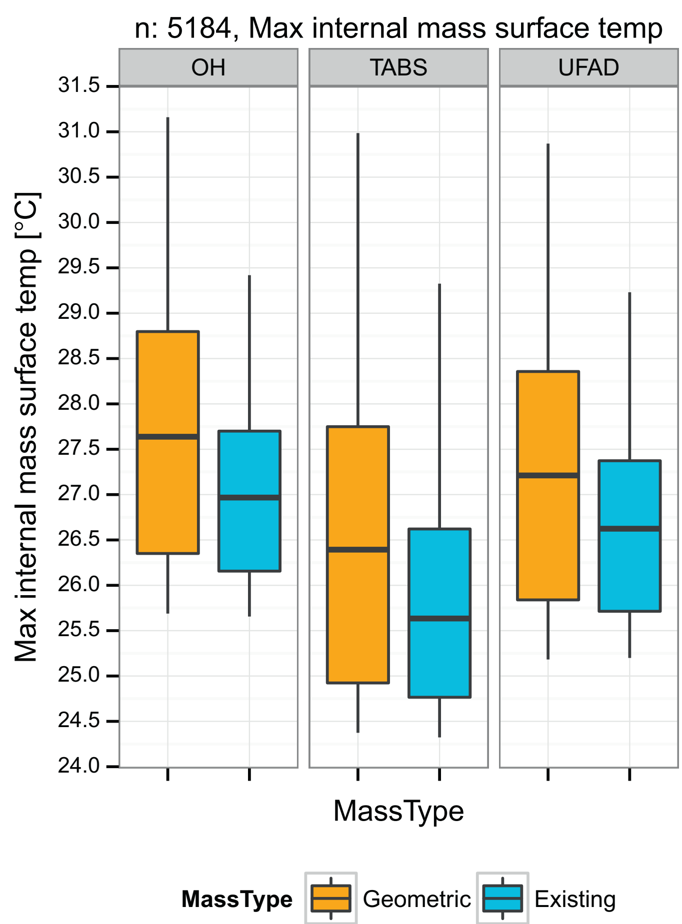


**Fig. 7.** Boxplot of peak surface temperatures of the internal mass for the entire dataset.

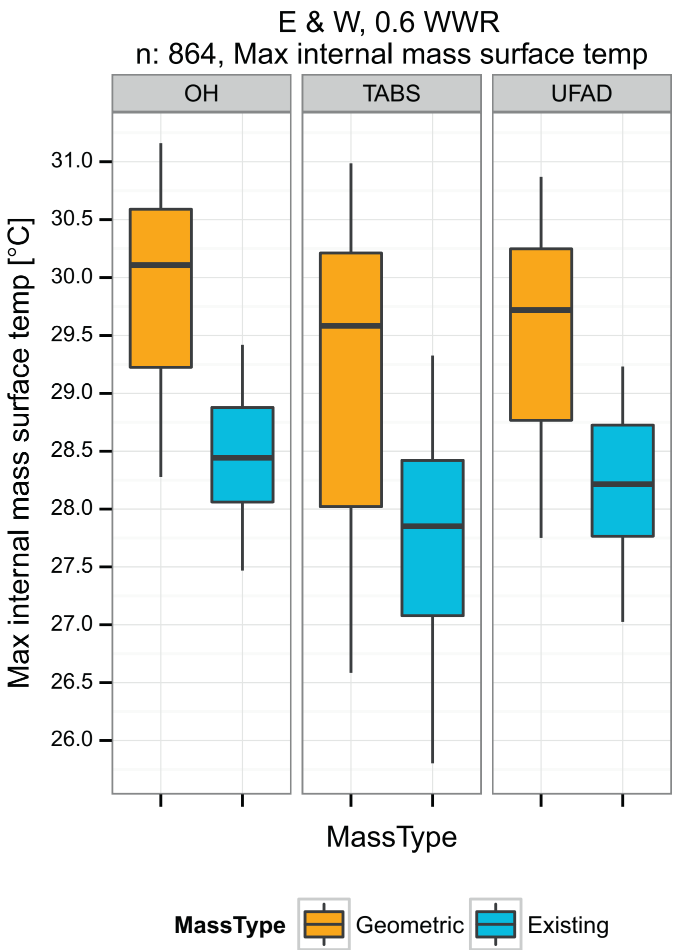


**Fig. 8.** Boxplot of peak surface temperatures of the internal mass for the high direct solar subset.

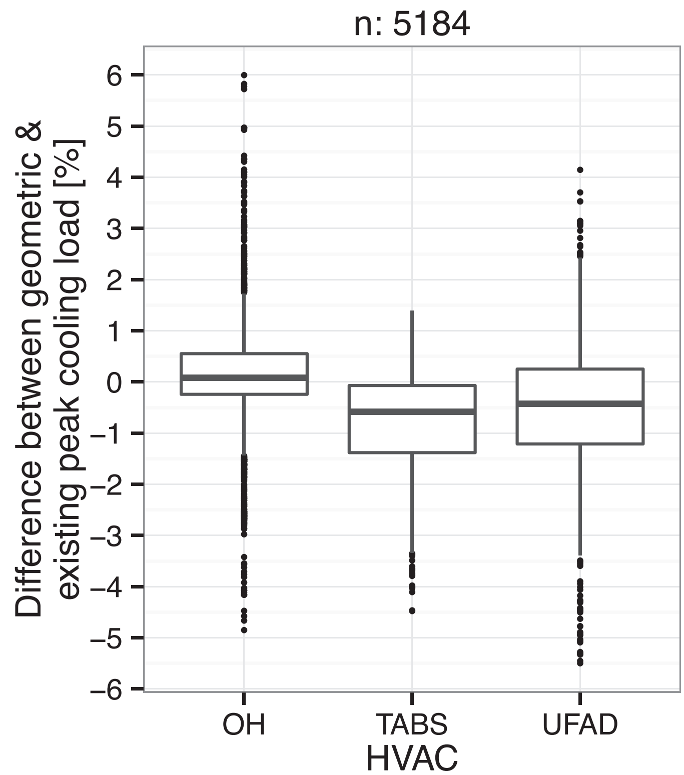


**Fig. 9.** Boxplot of difference in peak cooling load (existing – geometric) with respect to HVAC system.

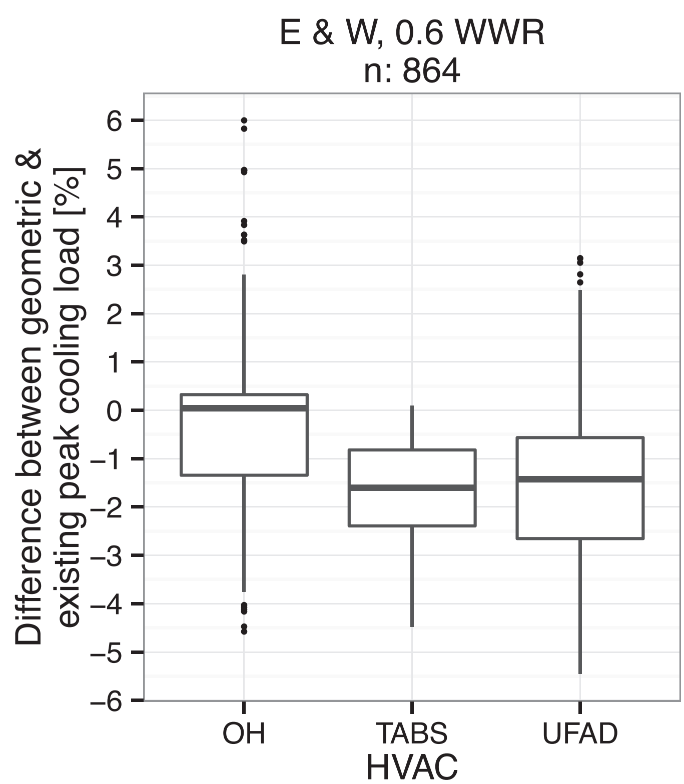


**Fig. 10.** Boxplot of difference in peak cooling load with respect to HVAC system for the high solar load subset.

parameter space. Working from the assumption that the parameter space is a reasonable representation of load cases in typical buildings, then modeling the furniture as geometric mass does not have a major impact on cooling load. However, the entire parameter space includes a large number of simulations in which there are low levels of direct solar radiation (e.g. north facing zones). As expected in this subset of runs, little change in peak load results from the choice of internal mass modeling method, as direct solar radiation is the primary difference between the two methods. The peak cooling load in the geometric cases changes by +0.01% (−0.12%, +0.22%) in this subset.

The "Geometric" modeling method has a larger effect −1.08% (−2.32%, 0.00%) in cases with high direct solar radiation (e.g. East and West facing zones with a large amount of fenestration). Fig. 10 illustrates this subset, broken out by HVAC system. As both Figs. 9 and 10 show, it is interesting to note that the choice of internal mass modeling method has a larger impact for HVAC systems that produce a surface temperature asymmetry within the zone (such as UFAD and TABS). In the high solar cases, the effect was larger −1.58% (−2.40%, −0.71%) for the UFAD & TABS cases.

Fig. 11 provides an overview of the impact that the amount of internal mass in the model has on peak cooling load, so that it may be of use for engineers and other researchers. Though the median effect is relatively low, the *range* of values clearly show that further research is needed to determine the amount of internal mass, its average thickness, and a representative set of material

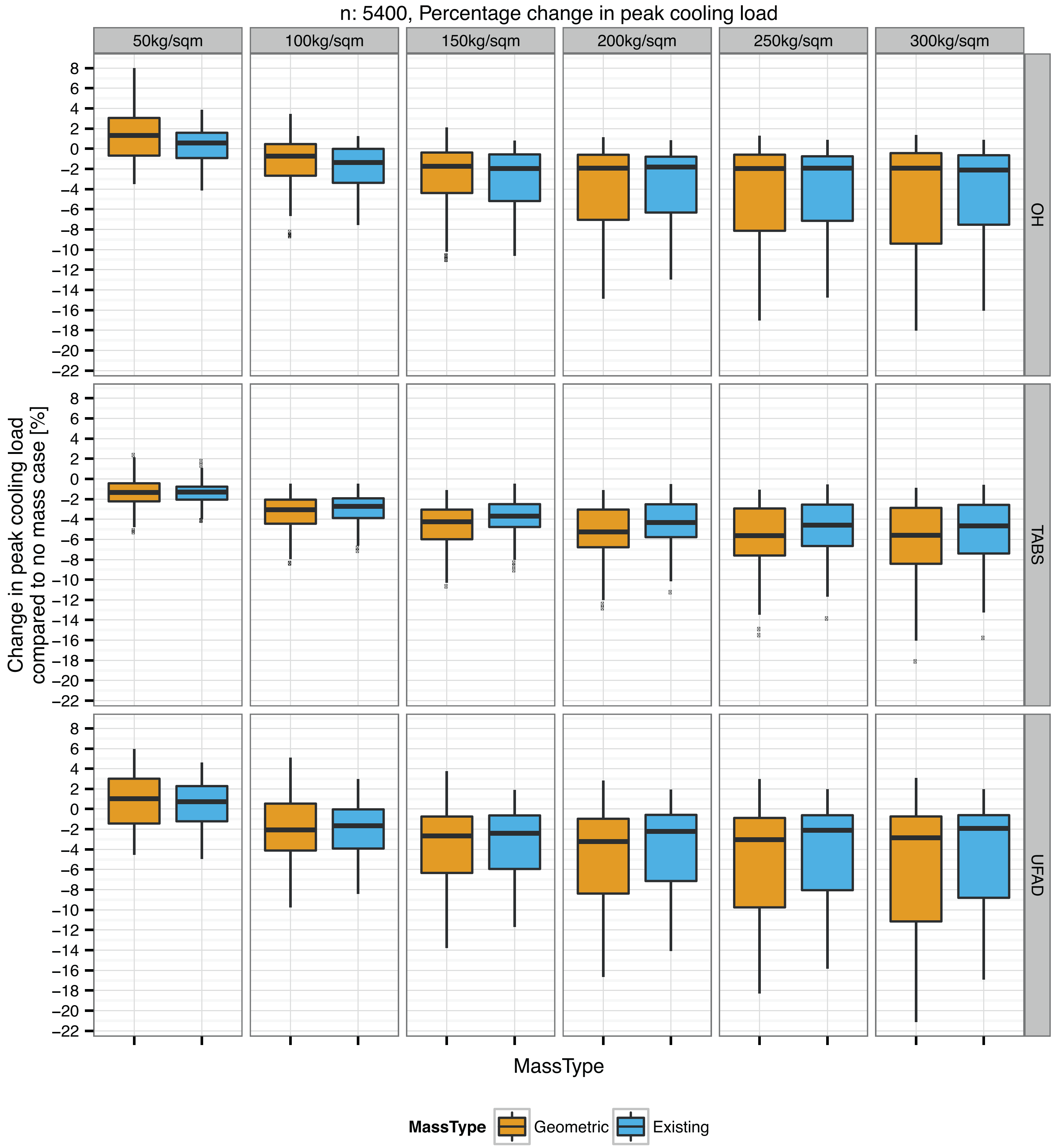


**Fig. 11.** Boxplot of change in peak cooling load compared to the no mass case with respect to the amount of internal mass and the type of HVAC system.

properties in typical building spaces, so that there is an experimental basis for the values used in whole building energy simulation models.

*4.3.3. Comparison of UFAD and overhead peak cooling loads*

Although it was not the primary aim of this study, we also directly compared the peak cooling loads for the OH and UFAD systems. Across all of the UFAD and OH cases, the UFAD cases have a 20.8% higher median peak cooling load ($n$: 3600), even though all parameters are identical other than those directly related to the supply air distribution method (i.e., the presence of a supply air plenum, a shorter return plenum, and a higher supply air temperature). The increased peak cooling load results from the presence of the raised floor in the UFAD case, which isolates the zone from the concrete slab and its associated thermal inertia. This is a comparable finding to a previous study which found a median 19% increase in peak cooling load when comparing UFAD to OH cases across 87 simulations of an 18 zone building [27].

## 5. Discussion

### 5.1. How much internal mass is 'right'?

After a thorough literature review, we were unable to find any published experimental (or theoretical) research regarding the recommended values for internal mass in models.[3] The only modeling guidance document that we found which explicitly prescribes an amount of internal mass (in IP units) was the California Nonresidential Alternative Calculation Method Manual (2005): 391 kg/m$^2$ or 80 lb/ft$^2$. This represents a quantity of internal mass that covers the entire zone floor area to an average thickness of 72 cm (2.4 ft) – assuming wood with a density of 540 kg/m$^3$ (34 lb/ft$^3$) as the material. Intuitively, this seems to be an unreasonably high value to represent furniture in most buildings (even if it includes an estimate for the mass of internal partitions when multiple rooms are lumped into one zone in the model). We assume these values stem from assumptions that are relevant to older simulation engines (such as DOE-2) that may not have accounted for the mass of the building structure (i.e. the slab) within the zone surface constructions. As more modern tools (such as EnergyPlus and ESP-R) inherently account for this, using these values effectively accounts for building structural mass twice, and is an inaccurate representation of the mass for the building.

Other, more recent sources, like the example benchmark commercial buildings from the PPNL [24] and earlier DOE [28] models, use 0.15 m (6 in.) of wood spread over twice the floor area of each zone. As this uses the existing internal mass object in EnergyPlus, it is exposed on only one side, and thus represents an internal mass object to a thickness of 0.3 m (1 ft) covering the entire floor area of each zone, or 177 kg/m$^2$ (assuming wood with a density of 540 kg/m$^3$ (34 lb/ft$^3$) as the material). This also seems a little high to the authors, but much closer to the realm of feasibility. The reader will note that the parameter values evaluated in this paper cover the range from 0 kg/m$^2$ to 300 kg/m$^2$ in 50 kg/m$^2$ increments.

Likewise, the same uncertainty surrounds the thickness of the internal mass used in the model. As demonstrated in Section 4.2.4, the thickness of the internal mass affects the results, even for a fixed amount of mass. However, as far as we are aware there has been no research published regarding what thickness is a realistic simplification of furniture and contents in a zone. As the thinnest dimension of a piece of furniture is typically at least 10 mm (e.g. a partition between two open office spaces, or the surface of a light desk), and typically at most 500 mm (e.g. a desk drawer, or a filing cabinet), the average must lie within this range. We estimate that 100–300 mm represents a reasonable average thickness for furniture in a typical office. This translates to an internal mass surface of half that range (50–150 mm) as the internal mass surfaces are adiabatic on one side in both the geometric and existing modeling methods.

## 6. Conclusion

In this study, we assessed the change in peak cooling load caused by adding internal mass (representing furniture and contents) to whole-building energy simulation models. We did this using a full factorial parametric study of 5400 EnergyPlus simulations. These simulations represent the wide range of load conditions expected in a typical office building. We presented a new method for modeling internal mass that more realistically captures modes of heat transfer within the zone by accounting the effect of direct solar radiation incident on an internal mass surface.

We presented the results using the median value following by the lower and upper quartiles in parentheses. Overall, we found that adding internal mass changed peak cooling load by −2.28% (−5.45%, −0.67%) across the studied parameter space. We determined that applying the new "Geometric" method changed peak cooling load by −0.25% (−1.02%, +0.23%) when compared to the existing method across all of the cases with mass in the studied parameter space. The "Geometric" modeling method has a larger effect −1.08% (−2.32%, 0.00%) in cases with high direct solar radiation (e.g. east and west facing zones with a large amount of fenestration), and almost no effect +0.01% (−0.12%, +0.22%) in zones with low solar loads (north facing zones). In the high solar cases, the effect was higher again −1.58% (−2.40%, −0.71%) for HVAC systems that yield a surface temperature asymmetry within the zone (such as UFAD and TABS). As part of this study we also noted an interesting result related to internal mass regardless of the modeling method used. The thickness of the internal mass surface added to the model has a relatively large impact on results, even when the amount of mass remains the same. When the mass is represented using relatively thin surfaces, it can actually increase peak cooling loads (Section 4.2.4).

Overall, we determined that the choice of modeling method is far from being the most significant parameter given the uncertainty in the other input parameters – particularly when taking the lack of solid guidance regarding how much internal mass to model, over what area, and what material to use. However, the geometric method should be considered in cases with high levels of direct solar radiation, high amount of internal mass, or for HVAC systems that cause a large temperature asymmetry in the zone.

Upon completion of this study, we realized that there is a different way to improve upon the existing method that would allow users the flexibility to explore how direct solar on internal mass impacts their model, but that would be easier to implement and use. By modifying the existing Internal Mass object in EnergyPlus (the existing method) to allow a user-defined portion of the direct solar radiation to be incident on the internal mass (e.g. 25–75%) instead of on the other surfaces in the model. This would capture both the effects of direct solar incident on furniture, and the partial shading of other surfaces in the zone, but would not require (a) adding an internal mass surface with a geometric description and (b) splitting the floor surface into three sub-surfaces. The user would once again have an additional parameter to use related to internal mass without experimental data to support the choice of a reasonable value, which is not ideal, but overall this would allow users the flexibility to explore this effect as needed.

This simulation study highlights the range impacts that internal mass can have on peak cooling loads in buildings depending on the parameters used, while the literature review highlights the lack of guidance on selecting reasonable parameter values. Based on this we recommend further research in the form of an experimental study to answer outstanding questions regarding internal mass in buildings: (1) How much internal mass is typical in buildings, and what is its distribution? (2) What is a reasonable value the average thickness of internal mass in aggregate? (3) What type of material best represents the aggregate properties of internal mass?

## Acknowledgement

The California Energy Commission PIER Buildings Program provided the funding for this research as part of the Advanced Integrated Systems Technology Development (CEC Contract 500–08-044).

[3] If a reader has information about such a study, we would appreciate feedback in this regard.

## References


[1] J. Clarke, Energy Simulation in Building Design, second ed., Routledge, Oxford, 2001.

[2] J. Seem, Modeling of heat transfer in buildings (Doctorate), University of Wisconsin, 1987.

[3] D.B. Crawley, L.K. Lawrie, F.C. Winkelmann, W.F. Buhl, Y.J. Huang, C.O. Pedersen, et al., EnergyPlus: creating a new-generation building energy simulation program, Energy and Buildings 33 (2001) 319–331, http://dx.doi.org/10.1016/S0378-7788(00)00114-6.

[4] B. Todorovic, Furniture of air-conditioned room and cooling load, in: Proc. 6th REHVA Int. Congr., REHVA, Milan, Italy, 1975.

[5] M.R. Shaw, K.W. Treadaway, S.T.P. Willis, Effective use of building mass, Renewable Energy 5 (1994) 1028–1038, http://dx.doi.org/10.1016/0960-1481(94)90130-9.

[6] Y. Zhang, K. Lin, Q. Zhang, H. Di, Ideal thermophysical properties for free-cooling (or heating) buildings with constant thermal physical property material, Energy and Buildings 38 (2006) 1164–1170, http://dx.doi.org/10.1016/j.enbuild.2006.01.008.

[7] L. Yang, Y. Li, Cooling load reduction by using thermal mass and night ventilation, Energy and Buildings 40 (2008) 2052–2058, http://dx.doi.org/10.1016/j.enbuild.2008.05.014.

[8] X. Xu, S. Wang, A simplified dynamic model for existing buildings using CTF and thermal network models, International Journal of Thermal Sciences 47 (2008) 1249–1262, http://dx.doi.org/10.1016/j.ijthermalsci.2007.10.011.

[9] F. Jiang, X. Wang, Y. Zhang, Analytical optimization of specific heat of building internal envelope, Energy Conversion and Management 63 (2012) 239–244, http://dx.doi.org/10.1016/j.enconman.2012.01.038.

[10] A. Jeanjean, R. Olives, X. Py, Selection criteria of thermal mass materials for low-energy building construction applied to conventional and alternative materials, Energy and Buildings 63 (2013) 36–48, http://dx.doi.org/10.1016/j.enbuild.2013.03.047.

[11] L.-S. Wang, P. Ma, E. Hu, D. Giza-Sisson, G. Mueller, N. Guo, A study of building envelope and thermal mass requirements for achieving thermal autonomy in an office building, Energy and Buildings 78 (2014) 79–88, http://dx.doi.org/10.1016/j.enbuild.2014.04.015.

[12] S. Wang, X. Xu, Parameter estimation of internal thermal mass of building dynamic models using genetic algorithm, Energy Conversion and Management 47 (2006) 1927–1941, http://dx.doi.org/10.1016/j.enconman.2005.09.011.

[13] R. Zeng, X. Wang, H. Di, F. Jiang, Y. Zhang, New concepts and approach for developing energy efficient buildings: ideal specific heat for building internal thermal mass, Energy and Buildings 43 (2011) 1081–1090, http://dx.doi.org/10.1016/j.enbuild.2010.08.035.

[14] US DOE, EnergyPlus Input/Output Reference v7.2, 2012, http://apps1.eere.energy.gov/buildings/energyplus/

[15] D.B. Crawley, J.W. Hand, M. Kummert, B.T. Griffith, Contrasting the capabilities of building energy performance simulation programs, Building and Environment 43 (2008) 661–673, http://dx.doi.org/10.1016/j.buildenv.2006.10.027.

[16] R. Henninger, M. Witte, D. Crawley, Analytical and comparative testing of EnergyPlus using IEA HVAC BESTEST E100-E200 test suite, Energy and Buildings 36 (2004) 855–863, http://dx.doi.org/10.1016/j.enbuild.2004.01.025.

[17] K.H. Lee, S. Schiavon, F. Bauman, T. Webster, Thermal decay in underfloor air distribution (UFAD) systems: fundamentals and influence on system performance, Applied Energy 91 (2012) 197–207, http://dx.doi.org/10.1016/j.apenergy.2011.09.011.

[18] B. Olesen, Radiant floor cooling systems, American Society of Heating, Refrigerating and Air-Conditioning Engineers, Inc. HVAC R Res. 50 (2008) 16–22.

[19] J. (Dove) Feng, S. Schiavon, F. Bauman, Cooling load differences between radiant and air systems, Energy and Buildings 65 (2013) 310–321, http://dx.doi.org/10.1016/j.enbuild.2013.06.009.

[20] K. Zhao, X.-H. Liu, Y. Jiang, Application of radiant floor cooling in a large open space building with high-intensity solar radiation, Energy and Buildings 66 (2013) 246–257, http://dx.doi.org/10.1016/j.enbuild.2013.07.014.

[21] F. Bauman, UFAD Guide: Design, Construction, and operation of Underfloor Air Systems, first ed., ASHRAE, 2013.

[22] ASHRAE, ASHRAE Standard 90.1-2007 Energy Standard for Buildings Except Low-Rise Residential Buildings, 2007.

[23] IESNA, Lighting Handbook: Reference & Application, eigth ed., Illuminating Engineering Society of North America, New York, USA, 1993.

[24] US DOE, DOE Commercial Building Reference Models, 2013, http://www.energycodes.gov/commercial-prototype-building-models

[25] US DOE, EnergyPlus Weather Data, 2014, http://apps1.eere.energy.gov/buildings/energyplus/weatherdata_about.cfm

[26] California Energy Commission, Nonresidential Alternative Calculation Method, 2013, http://www.energy.ca.gov/2013publications/CEC-400-2013-004/CEC-400-2013-004-SD.pdf

[27] S. Schiavon, K.H. Lee, F. Bauman, T. Webster, Simplified calculation method for design cooling loads in underfloor air distribution (UFAD) systems, Energy and Buildings 43 (2011) 517–528, http://dx.doi.org/10.1016/j.enbuild.2010.10.017.

[28] US DOE, Commercial Building Reference Models, 2010, http://energy.gov/eere/buildings/commercial-reference-buildings